



Original contribution

Docked severe acute respiratory syndrome coronavirus 2 proteins within the cutaneous and subcutaneous microvasculature and their role in the pathogenesis of severe coronavirus disease 2019



Cynthia M. Magro MD^{a,*,**}, J. Justin Mulvey MD, PhD^b,
Jeffrey Laurence MD^c, Surya Seshan MD^a, A. Neil Crowson MD^d,
Andrew J. Dannenberg MD^e, Steven Salvatore MD^a, Joanna Harp MD^f,
Gerard J. Nuovo MD^{g,*}

^a Department of Pathology and Laboratory Medicine, Weill Cornell Medicine, New York, NY 10065, USA

^b Department of Laboratory Medicine, Memorial Sloan-Kettering Cancer Center, New York, NY 10065, USA

^c Department of Medicine, Division of Hematology and Medical Oncology, Weill Cornell Medicine, New York, NY 10065, USA

^d Pathology Laboratory Associates and University of Oklahoma, Oklahoma City, OK 77069, USA

^e Department of Medicine, Division of Gastroenterology and Hepatology, Weill Cornell Medicine, New York, NY 10065, USA

^f Department of Dermatology, Weill Cornell Medicine, New York, NY 10065, USA

^g Ohio State University Comprehensive Cancer Center and Discovery Life Sciences, Columbus, OH 43065, USA

Received 18 August 2020; revised 30 September 2020; accepted 3 October 2020

Available online 12 October 2020

Keywords:

Complement;
Skin;
Deltoid biopsy;
SARS-CoV-2;
ACE2;

Summary The purpose of this study was to examine the deltoid skin biopsy in twenty-three patients with coronavirus disease 2019 (COVID-19), most severely ill, for vascular complement deposition and correlate this with severe acute respiratory syndrome coronavirus 2 (SARS-CoV-2) viral RNA and protein localization and ACE2 expression. Deltoid skin microvascular complement screening has been applied to patients with various systemic complement-mediated microvascular syndromes, best exemplified by atypical hemolytic uremic syndrome. In 21 of 23 cases, substantial microvascular

* Corresponding author. Ohio State University Comprehensive Cancer Center and Discovery Life Sciences, 1476 Manning Parkway, Powell, OHIO, 43065, USA.

** Corresponding author. Department of Pathology and Laboratory Medicine, Weill Cornell Medicine, 1300 York Avenue, F-309, New York, NY, 10065, USA.

E-mail addresses: cym2003@med.cornell.edu (C.M. Magro), nuovo.1@osu.edu (G.J. Nuovo).

COVID-19

deposition of complement components was identified. The two patients without significant complement deposition included one patient with moderate disease and a severely ill patient who although on a ventilator for a day was discharged after 3 days. The dominant microvascular complement immunoreactant identified was the terminal membranolytic attack complex C5b-9. Microvascular complement deposition strongly colocalized *in situ* with the SARS-CoV-2 viral proteins including spike glycoproteins in the endothelial cells as well as the viral receptor ACE2 in lesional and nonlesional skin; viral RNA was not evident. Microvascular SARS-CoV-2 viral protein, complement, and ACE2 expression was most conspicuous in the subcutaneous fat. Although the samples from severely ill patients with COVID-19 were from grossly normal skin, light microscopically focal microvascular abnormalities were evident that included endothelial cell denudement, basement membrane zone reduplication, and small thrombi. It is concluded that complement activation is common in grossly normal skin, especially in the subcutaneous fat which may provide a link between severe disease and obesity, in people with severe COVID-19, and the strong colocalization with the ACE2 receptor and viral capsid proteins without viral RNA suggests that circulating viral proteins (ie, pseudovirions) may dock onto the endothelial of these microvessels and induce complement activation.

© 2020 The Author(s). Published by Elsevier Inc. This is an open access article under the CC BY-NC-ND license (<http://creativecommons.org/licenses/by-nc-nd/4.0/>).

1. Introduction

We have recently demonstrated that complement-mediated microvascular injury is a critical feature that underlies the pathophysiology of severe coronavirus disease 2019 (COVID-19) and presented evidence that endocytosed spike glycoproteins of severe acute respiratory syndrome coronavirus 2 (SARS-CoV-2) within endothelium result in the direct activation of the mannan-binding lectin (MBL) complement pathway in the microvasculature of the lung and skin [1]. We showed that SARS-CoV-2–induced acute respiratory failure is a microangiopathy targeting the septal capillary microvasculature, whereby extensive microvascular deposits of C4d and C5b-9 suggest a causal association between complement deposition and vascular injury [1].

Based on World Health Organization (WHO) classifications for mild, moderate, severe, and critical disease [2] (in this document, critical and severe will be combined as *severe*), patients with severe COVID-19 have evidence of other organ dysfunction related to complement-mediated and prothrombotic vascular disease such as stroke, hepatic failure, lower extremity arterial occlusion, and acute kidney injury (AKI) [3,4]. In the skin, this pathobiology underlies the distinctive COVID-19–associated thrombotic retiform purpura, corresponding microscopically with a complement-mediated pauci-inflammatory thrombogenic vasculopathy [1,5].

A deltoid skin biopsy has been used to diagnose patients with other systemic complement-mediated microvascular injury syndromes such as atypical hemolytic uremic syndrome (aHUS) and differentiate these disorders from thrombotic thrombocytopenic purpura associated with antibodies to ADAMSTS13 (a disintegrin and metalloproteinase with a thrombospondin type 1 motif, member 13) [6]. This procedure has been performed at our

institution to determine suitability for complement inhibition therapy with the humanized monoclonal antibody eculizumab, which targets the terminal complement component C5.

In the initial pilot study of five COVID-19 cases [1] wherein complement-mediated vascular injury was seen in severe COVID-19, we were able to document evidence of systemic complement activation using the deltoid biopsy in two patients. Since then, we have been using the established normal skin biopsy protocol to identify ill patients who might benefit from complement inhibition therapy when refractory to other therapies.

This manuscript provides a detailed analysis of SARS-CoV-2 viral protein, ACE2, SARS-CoV-2 viral RNA, and complement deposition patterns in skin from patients with severe and fatal COVID-19. The data suggest that circulating pseudovirions are endocytosed by ACE2+ endothelial cells in the skin's microvessels that can induce localized MBL complement activation and therefore define a potential mechanism for distant microvascular and prothrombotic complications owing to the interplay and amplification of MBL activation with the alternative complement pathway and coagulation cascade.

2. Materials and methods

2.1. Biopsy material

The patient cohort (cases 1 through 23) included archival biopsy material of normal-appearing deltoid skin procured from 14 live patients who were significantly symptomatic with COVID-19 (cases 1 through 14) and from 9 people who died of the disease. The normal skin biopsies were performed by the attending dermatologist at the request of the treating physician to establish evidence of systemic involvement of significant complement activation

providing justification for use of eculizumab in those cases not responding to current therapy. Thirteen of these patients fulfilled the Centers for Disease Control and Prevention (CDC) criteria to be labeled as having severe COVID-19, whereas one patient was designated as having moderate COVID-19. The categorization as moderate and severe was based on criteria set forth by the World Health Organization (WHO). Moderate COVID-19 is defined by an infected patient with fever and who is bedridden, exhibiting variable shortness of breath although not requiring intensive care hospitalization with ventilator support, whereas patients falling into the severe COVID-19 category have organ failure typically the lung or kidney and require intensive care hospitalization. Three of these patients are part of a previously published study [1]. In each of the 23 cases, there was confirmation of SARS-CoV-2 infection with a positive nasopharyngeal swab result for SARS-CoV-2 RNA.

2.1.1. Control group

Also studied from a vascular complement deposition perspective was normal skin in patients in the pre-COVID-19 era not known to have systemic complement activation. Specifically, six grossly normal deltoid biopsies obtained from patients of the pre-COVID-19 era who had undergone deltoid biopsy to rule out aHUS were studied; each patient was found not to have aHUS based on the overall clinical presentation and laboratory parameters. Eight additional blocks of deltoid skin procured from routine re-excision specimens from the pre-COVID era were also assessed. Finally, skin samples taken for conditions unrelated to COVID-19 were obtained from four patients who were COVID-19 positive but without clinical features of moderate or severe COVID-19.

The samples were first examined by routine hematoxylin and eosin staining. The focus of the study was the evaluation of the vascular deposition of C5b-9, C3d, and C4d with SARS-CoV-2 localization. In some of the biopsies, we also assessed MBL-associated serine protease-2 (MASP2).

2.2. Evaluation of complement deposition

Significant C5b-9 deposition was defined as a vaso-centric granular and/or homogeneous pattern well above the background at least of moderate intensity, typically in an endothelial and/or subendothelial location. An evidence-based cutoff of fewer than 10 positive-staining vessels was not considered diagnostic of significant complement deposition. Other nondiagnostic patterns included C5b-9 deposits within the epidermal and eccrine coil basement membrane zone, the pilar erector muscle and dermal elastic fibers, the internal elastic lamina of vessels, and elastic tissue around lymphatics. The other markers of

complement were assessed by the same principles applied for C5b-9. The methodologies for C3d, C4d, and C5b-9 staining have been described in prior publications [7,8]. Immunohistochemical staining of C3d (ready-to-use polyclonal antibody; Cell Marque, Rocklin, CA, USA), C4d (1:50, monoclonal antibody; Quidel, San Diego, CA, USA), and C5b-9 (1:250, clone aE11; Dako, Santa Clara, CA, USA) was accomplished using the Bond III Autostainer (Leica Microsystems, Illinois, USA). Formalin-fixed and paraffin-embedded tissue sections were first baked and deparaffinized. Antigen retrieval was followed by heating the slides at 99–100 °C in Bond Epitope Retrieval Solution 2 (Leica Biosystems, Buffalo Grove, IL, USA) for 20 min (for C3d and C4d) and at 37 °C in Bond Enzyme solution for 10 min (for C5b-9). The sections were then incubated sequentially with the primary antibody for 15 min, post-primary antibody (equivalent to the secondary antibody) for 8 min, polymer (equivalent to the tertiary antibody) for 8 min, endogenous peroxidase block for 5 min, diaminobenzidine (DAB) for 10 min, and hematoxylin for 5 min. The Bond Polymer Refine Detection kit (Leica Biosystems, Buffalo Grove, IL, USA) was used for all three antibodies. The material reviewed for this study represents archival pathology material, wherein any additional studies were covered under IRB protocol 20-02021524.

2.3. In situ hybridization

Detection of SARS-CoV-2 RNA was carried out using the ACD (Newark, CA, USA) RNAscope probe (cat no. 848561-C3) through a previously published protocol in which only the viral RNA probe is changed [12,13]. The SARS-CoV-2 probe targets the region nt 21631 - 23303 derived from the genomic sequence of the virus (NC_045512.2). In brief, pretreatment in the ACD RNA retrieval solution and protease digestion is followed by overnight hybridization at 37 °C and detection using the ACD 2.5 HD DAB detection kit.

2.4. Immunohistochemistry

Our immunohistochemistry protocol for SARS-CoV-2 capsid proteins has been previously published in the studies by Nuovo [9,13] and Nuovo et al [12]. In brief, the Leica Bond Max automated platform (Leica Biosystems, Buffalo Grove, IL, USA) was used with the primary antibodies (ProSci, Poway, CA) at dilutions of 1:250 (membrane), 1:4500 (spike), and 1:500 (envelope) after antigen retrieval for 30 min. The horseradish peroxidase (HRP) conjugate from Enzo Life Sciences (Farmingdale, NY, USA) was used in place of the equivalent reagent from Leica as this has been shown to substantially reduce background [9]. We also assessed ACE2 expression using the primary antibody

Table 1 Clinical summary of COVID-19–positive patients.

| Case | Age | Sex | Skin lesion | BMI | Prolonged ventilator dependent | AKI | Mortality |
|------|-----|-----|---------------|------|--------------------------------|-----|-----------|
| 1 | 73 | M | AL(p) | 34.1 | + | + | + |
| 2 | 66 | F | AL(p/p) | 27.7 | + | + | + |
| 3 | 36 | F | AL(p) | 22.1 | + | - | - |
| 4 | 70 | M | AL | 23.1 | + | + | - |
| 5 | 40 | F | AL/torso L | 23.4 | + | - | - |
| 6 | 71 | M | AL(P) | NA | + | + | + |
| 7 | 52 | M | - | 31.4 | - | + | - |
| 8 | 33 | F | - | 22.4 | - | - | - |
| 9 | 62 | M | - | NA | + | + | - |
| 10 | 30 | F | - | NA | + | + | - |
| 11 | 72 | M | - | NA | + | + | + |
| 12 | 73 | F | - | 32.9 | - | - | - |
| 13 | 43 | M | - | 34.1 | + | + | - |
| 14 | 28 | M | - | 37.2 | + | - | - |
| 15 | 56 | F | None | 25.7 | + | - | + |
| 16 | 73 | M | None | 32.9 | - | - | + |
| 17 | 46 | M | None | NA | + | + | + |
| 18 | 69 | M | None | 31.6 | - | - | + |
| 19 | 34 | M | None | 43 | + | + | + |
| 20 | 95 | F | None | 19.7 | - | - | + |
| 21 | 79 | M | None | 31.8 | - | + | + |
| 22 | 64 | M | None | 22.3 | - | - | + |
| 23 | 69 | M | None | 27.3 | + | + | + |

NOTE. Cases 1–14 were alive, and all had severe COVID-19, excluding case 12 who had moderate COVID-19; cases 15–23 represent patients who died from fatal COVID-19.

Abbreviations: AKI, acute kidney injury; BMI, body mass index; AL, acral livedo; L, livedo; NA, not available; COVID-19, coronavirus disease 2019.

from Proteintech (Chicago, IL, USA) (1: 13,000 dilution, antigen retrieval for 30 min).

2.5. Coexpression analysis

Coexpression analyses were carried out using the Nuance system (Hebron, KY, USA), whereby each chromogenic signal is separated, converted to a fluorescence based signal, and then mixed to determine if cells were expressing the two proteins of interest [9,10].

2.6. Electron microscopy

Electron microscopy was performed on deparaffinized tissue from deltoid skin in the routine manner using osmium tetroxide and stained with uranyl acetate and lead citrate. Ultrastructural photography was performed by transmission electron microscopy (HT-7800, Santa Clara CA, USA).

3. Results

3.1. Clinical features

Six female and eight male patients diagnosed with moderate ($n = 1$) or severe ($n = 13$) COVID-19, with a positive reverse transcriptase polymerase chain reaction (RT-PCR) assay for SARS-CoV-2, as performed at a designated laboratory, and ranging in age from 28 to 73 years, had skin biopsies taken from the deltoid region. These are shown as cases 1–14 in Table 1. Twelve of the 14 patients were in respiratory failure on a ventilator, although one patient (case 8) was extubated 1 day after the biopsy was performed and was discharged to home 3 days later. One patient (case 7) with sickle cell anemia developed AKI without respiratory failure, and 8 others also had AKI (Table 1). One patient (case 12) had significant respiratory symptoms but neither was on a ventilator at the time of biopsy nor did the patient subsequently become ventilator dependent or develop any acute organ failure. This patient fulfilled criteria to warrant categorization as being moderately ill with COVID-19. Six of the severely ill patients on ventilator support had livedoid skin rashes (cases 1 through 6), involving the extremities with prominent acral localization in 4 patients and the torso in 1 patient (Fig. 1A) (Table 1); 3 of the 6 patients died. Among pre-existing conditions were hypertension (1), pulmonary hypertension (1), prostate cancer (1), diabetes mellitus (1), sickle cell anemia (1), fibrosing mediastinitis (1), pulmonary atresia (1), and deep venous thrombosis (1). In addition, the patient's body mass indices (BMIs) ranged from 22.1 to 37.2 although data were unavailable for 4 of 14 cases. In the cases where data were available, 5 of 10 (50%) of the patients would be categorized as obese based on a BMI in excess of 30.

The 9 autopsy cases (cases 15–23 in Table 1) comprised 7 men and 2 women, ranging in age from 34 years to 95 years. All patients died from SARS-CoV-2–associated acute respiratory distress syndrome. Their clinical course was complicated by AKI in 4 of the 9 cases and acute liver injury in 1 case. Their initial presentation at the hospital was one of cough, fever, and progressive shortness of breath. The time that lapsed between presentation at the hospital with admission and death ranged from 1 day to 3 weeks. Pre-existing conditions were seen in all including hypertension (6), hyperlipidemia (4), diabetes mellitus (4), coronary artery disease (2), chronic lung disease (2), and malignancy (2) (Table 1). The patient's BMIs ranged from 19.7 to 43, with an average BMI of 28.8; 4 of 9 patients were obese. None of these patients had a skin rash.

3.2. Complement deposition in microvessels

Although the dominant focus of this study was normal deltoid skin, in 6 of the cases, there was a biopsy performed of the livedoid rash of COVID-19. The biopsied livedoid

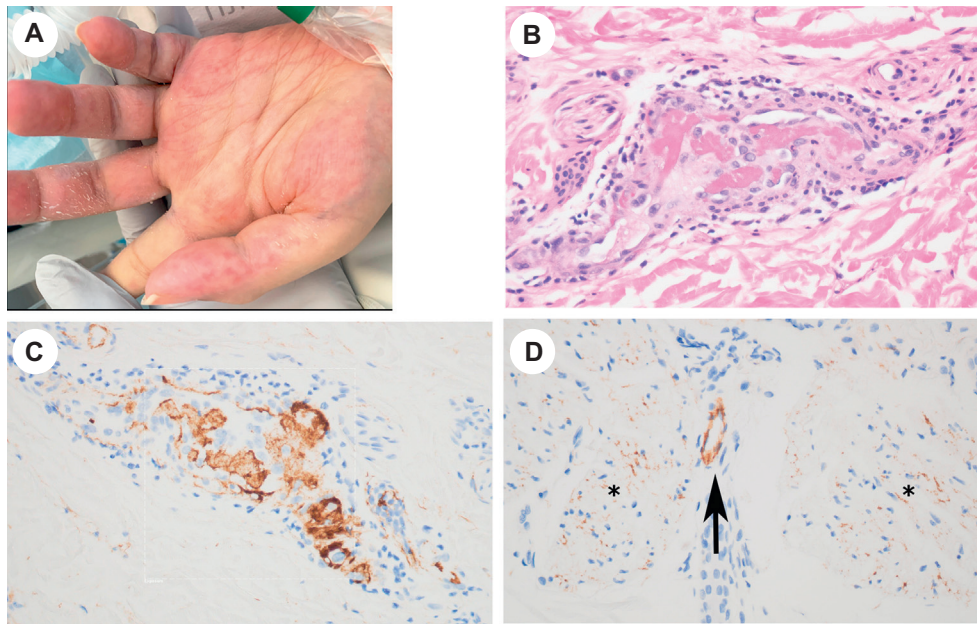


Fig. 1 Thrombotic retiform purpura of COVID-19 is a complement-mediated microvascular injury reflective of systemic complement activation. The patient is a 36-year-old woman with COVID-19—associated acute respiratory distress syndrome (ARDS) who presents with classic acral livedo (case 3) (A). The biopsy of lesional acral skin showed a pauci-inflammatory thrombotic vasculopathy affecting the venous and arterial system (H&E, $\times 400$) (B). There are extensive deposits of C5b-9 within the vessel wall. The deposits are conspicuous in the vascular lumen, in the endothelium, and abluminally. A similar deposition pattern was observed for C3d and C4d (not illustrated) (diaminobenzidine, $\times 400$) (C). The deltoid skin biopsy shows significant vascular deposits of C5b-9. Illustrated is the typical endothelial and abluminal staining pattern that defines a positive reaction in a vessel (arrow). Note the nonspecific staining pattern in the pilar erector muscle (asterisk) (diaminobenzidine, $\times 400$) (D). COVID-19, coronavirus disease 2019; H&E, hematoxylin and eosin.

rash showed a pauci-inflammatory thrombotic vasculopathy affecting capillaries and both the venous and arterial systems. There was morphologic evidence of endothelial cell injury. The thrombotic diathesis was largely unaccompanied by significant inflammation. There were extensive vascular deposits involving capillaries and the venular and arterial system throughout the dermis and subcutaneous fat for C5b-9 (Fig. 1B, C, and D, Fig. 6), C3d, and C4d.

Normal deltoid skin biopsies from 11 of 14 premortem cases, including all 6 cases with biopsied livedoid rashes, showed significant deposits of C5b-9 within vessels especially vessels in the mid, deeper dermis and subcutaneous fat in excess of 10 positive staining vessels. Vascular decoration for C4d, although positive in 12 of 14 cases, was significantly less in terms of the number of positive vessels and intensity of decoration, except in two cases wherein it exceeded vascular decoration for C5b-9. C3d exhibited positive immunoreactivity in 8 of 14 cases, but was qualitatively and quantitatively less than that observed for C5b-9, except in 1 case.

In 11 of 14 cases, the vascular complement deposition was present in capillaries, venules, and the arterial system. Two of the 3 cases without arterial complement decoration had less severe disease (case 8 and case 12).

In cases 8 and 12, the number of vessels expressing any of the complement components was not deemed to be significant as it was less than 10 vessels with a positive reaction. One had a moderate disease course and did not require ventilation at any point during her clinical course. Case 8 did not require prolonged ventilation.

MASP2, a marker of MBL pathway complement activation, was positive in 4 of 7 cases that were evaluated and exhibited an endothelial and intravascular deposition pattern (Fig. 2B), whereas it was negative in one patient without severe COVID-19 (case 8).

3.3. In situ detection of viral capsid proteins and RNA

Fourteen of the 23 biopsies wherein tissue was available were tested for SARS-CoV-2 viral RNA as well as the capsid protein envelope, spike, and/or membrane by immunohistochemistry and compared with normal skin biopsies obtained before 2018 ($n = 10$); the results were read blinded to the clinical information. In each of the severe COVID-19 cases represented by biopsies of thrombotic retiform purpura and normal-appearing deltoid skin, viral protein was detected in microvessels especially in the mid to deep dermis and subcutaneous fat (Fig. 2A through

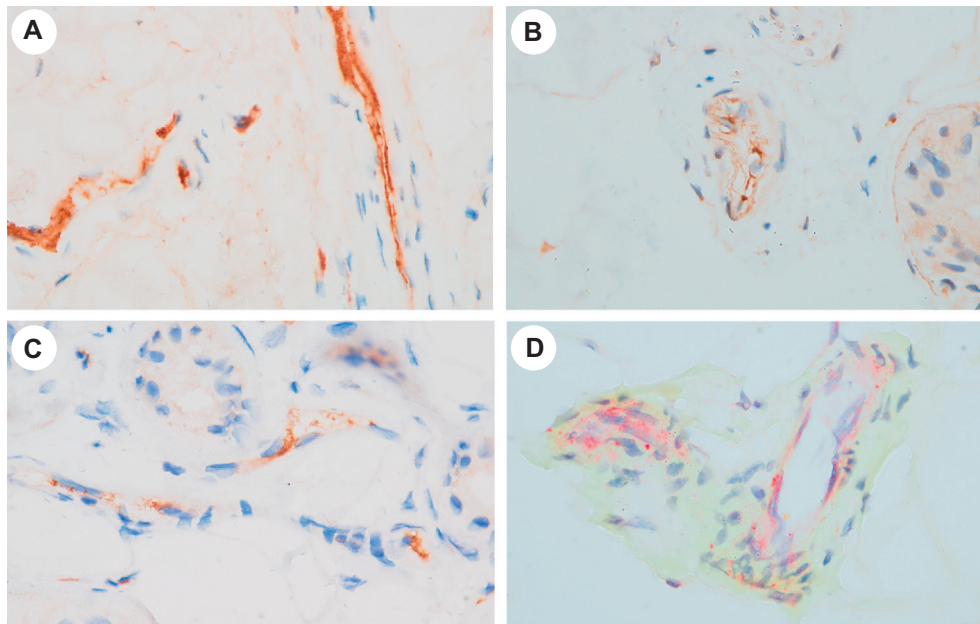


Fig. 2 Molecular correlates of SARS-CoV-2 protein docking in the endothelia of the microvessels of the dermis/subcutaneous fat from 4 different patients with severe COVID-19 complicated by microangiopathic ARDS. A biopsy of thrombotic retiform purpura demonstrates prominent cytoplasmic expression of SARS-CoV-2 envelope protein (diaminobenzidine, $\times 1000$) (A). A biopsy of nonlesional deltoid skin demonstrates cytoplasmic immunoreactivity for SARS-CoV-2 membrane protein within endothelial cells lining capillaries and venules (diaminobenzidine, $\times 1000$) (B). A biopsy of nonlesional deltoid skin shows prominent endothelial cell expression of SARS-CoV-2 envelope protein within microvessels (C). A biopsy of deltoid skin shows significant expression of SARS-CoV-2 spike glycoprotein in the microvasculature of the subcutaneous fat (red chromogen, $\times 1000$) (D). COVID-19, coronavirus disease 2019; SARS-CoV-2, severe acute respiratory syndrome coronavirus 2; ARDS, acute respiratory distress syndrome.

D). Each of the negative controls was negative for SARS-CoV-2 capsid proteins. Serial section analyses showed that the SARS-CoV-2 capsid proteins showed equivalent distributions, including the parallel microvascular expression pattern being noted for the spike glycoprotein (S) and membrane protein (M) of SARS-CoV-2 although spike glycoprotein expression was qualitatively and quantitatively less than viral capsid membrane and or envelope expression. Coexpression analyses also confirmed that the endothelial expression of the complement-activated proteins colocalized with the viral capsid proteins in 3 cases tested (Fig. 5A and B).

Additional serial sections were then tested for SARS-CoV-2 RNA using *in situ* hybridization. All COVID-19 skin biopsies tested were negative for viral RNA, with strong positive controls from the lung tissues of people who died of COVID-19.

3.4. Detection of the ACE2 receptor

Because the receptor for SARS-CoV-2 is ACE2, the skin biopsy cases and controls were tested for ACE2 by immunohistochemistry, whereby a total of 15 cases were examined (10 study cases and 5 normal controls). Endothelial cells, especially in the lower dermis and subcutaneous fat, strongly expressed the ACE2 receptor, in both the COVID-19 cases and negative controls (Fig. 3A and B).

Coexpression analyses on the select studied COVID-19 cases confirmed that ACE2 colocalized with both the viral capsid proteins and the endothelial marker CD31, wherein it was most prominent in the microvasculature of the deeper dermis and subcutaneous fat than in the superficial dermis. Larger caliber arteries were negative for ACE2 and viral capsid proteins. Colocalization was observed with CD31, the vascular marker, ACE2, and SARS-CoV-2 capsid proteins (Fig. 4A through C).

3.5. Complement and SARS-CoV-2 protein and complement in control specimens

None of the control specimens as outlined under the [Materials and methods](#) section showed significant deposition of C5b-9, C3d, and or CD4 (ie, less than 10 positive staining vessels). COVID-19—positive patients with mild or asymptomatic disease were negative for SARS-CoV-2 viral protein and the normal pre-COVID controls.

3.6. Histologic evidence of microvasculature damage in grossly normal skin in COVID-19

To assess if there was any morphologic evidence that the complement deposition was associated with any subtle evidence of microvascular injury, the samples were carefully scrutinized for the type of small vessel injury that

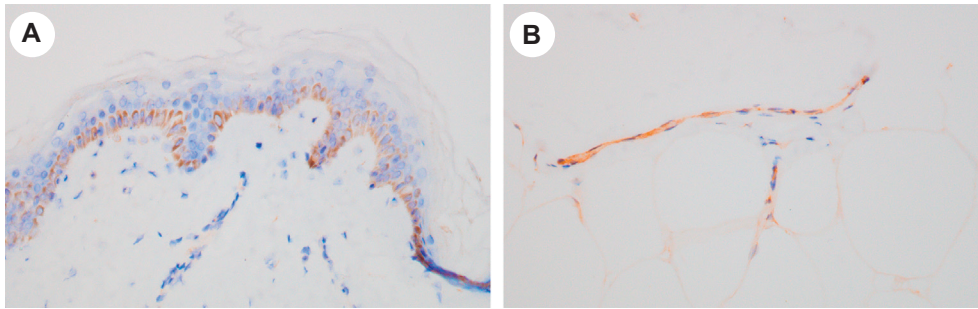


Fig. 3 Expression of ACE2 in the dermal and subcutaneous vasculature of normal deltoid skin in a patient who had fatal COVID-19–associated ARDS. There is a relative lack of expression of ACE2 in the endothelial cells of the microvessels of the superficial dermis (A). In contrast, there is strong expression of ACE2 within capillaries and venules of the subcutaneous fat (B). COVID-19, coronavirus disease 2019; ARDS, acute respiratory distress syndrome.

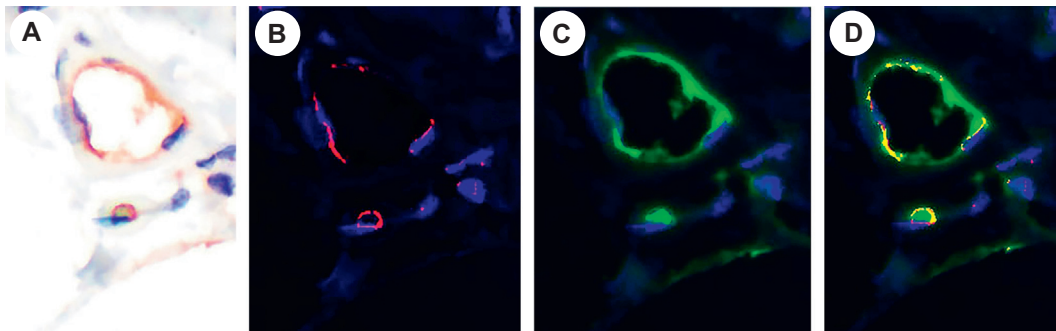


Fig. 4 Co-expression of ACE2 and SARS-CoV-2 capsid proteins with the cutaneous and subcutaneous microvasculature in a normal deltoid skin biopsy from a patient with fatal COVID-19–associated ARDS. Illustrated is a deep dermal venule exhibiting positive staining for ACE2 stained with a red chromogen and SARS-CoV-2 membrane protein stained with diaminobenzidine (A). Nuance software isolates ACE2 as fluorescent red (B) and the SARS-CoV-2 membrane as fluorescent green (C). Fluorescent yellow signifies areas of colocalization for ACE2 and SARS-CoV-2 membrane (D). COVID-19, coronavirus disease 2019; SARS-CoV-2, severe acute respiratory syndrome coronavirus 2; ARDS, acute respiratory distress syndrome.

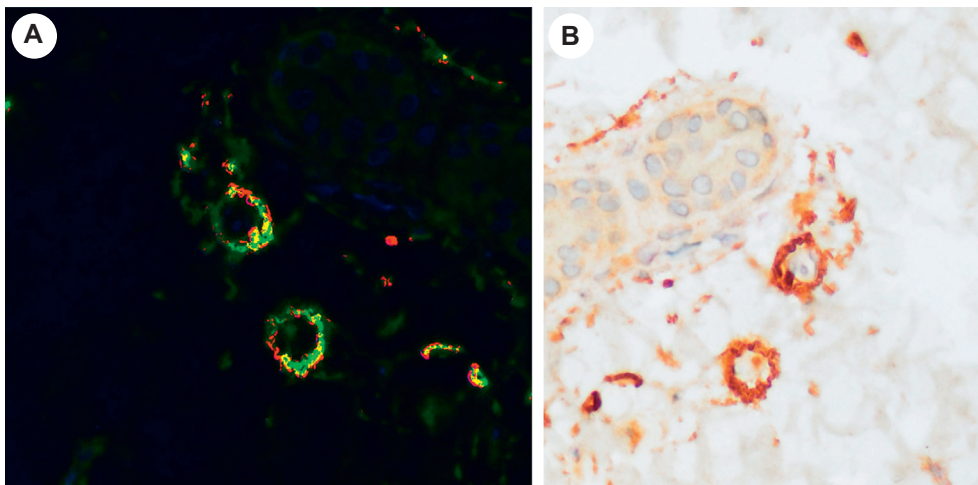


Fig. 5 There is striking colocalization of complement and SARS-CoV-2 protein within the microvasculature of the dermis and subcutaneous fat. In this postmortem normal deltoid skin biopsy, perieccrine blood vessels show expression of both C4d and spike glycoprotein. Using Nuance software, C4d exhibits a green immunoreactant staining pattern, whereas spike glycoprotein is red. The colocalized C4d and the SARS-CoV-2 spike glycoprotein produce a yellow (A) signal (C4d is stained with DAB, whereas the spike glycoprotein is stained with a red chromogen, $\times 400$) (B). DAB, diaminobenzidine.

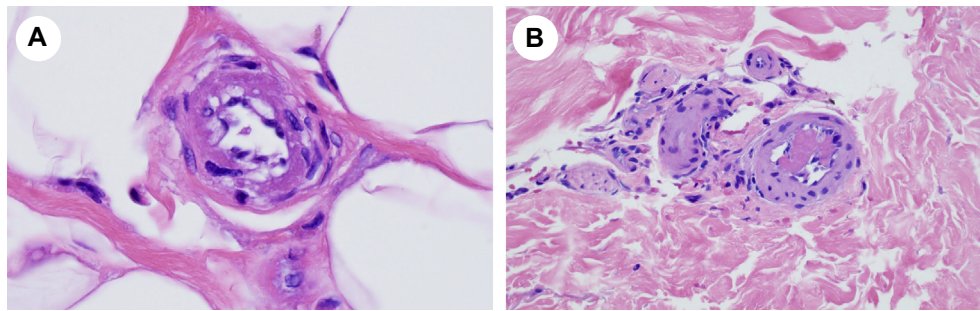


Fig. 6 Microvascular changes consistent with the sequelae of complement-mediated vascular injury localized within the fat. There is endothelial cell detachment involving an arteriole (A). Intraluminal thrombus formation was identified involving rare vessels and in the deeper dermis and subcutaneous fat either attributable to endothelial cell injury or reflective of a procoagulant state, which is also operational in these patients (B).

signifies complement-mediated injury. Primarily involving the deeper dermis and microvasculature of the fat, there was very focal endothelial cell denudement (Fig. 6A), basement membrane zone reduplication, aneurysmal dilatation of capillaries, and luminal thrombi (Fig. 6B); small foci of lipomembranous fat necrosis, presumably driven by local anoxia, were also noted. The changes were similar to the septal microangiopathy of severe COVID-19 but were only discernible with very careful inspection and by examining the vessels under oil immersion.

3.7. Ultrastructural analysis of normal skin

One case of autopsy deltoid skin was examined ultrastructurally. A deep dermal capillary showed endothelial cell swelling, abundant rough endoplasmic reticulum, intracytoplasmic lysosomes, and microvesicular bodies, representing a form of lysosomes that are associated with cellular injury. In addition, there were a cluster of circular bodies with indistinct spike-like projections emanating from the surface, ranging from 45 to 55 nm in diameter, without a granular core (arrow heads) and found freely within the cytosol (Fig. 7), which would represent clathrin coated vesicles or possibly pseudovirions. Intact virions were not identified.

4. Discussion

It was recently shown that complement-mediated microvascular injury affecting the septal capillaries of the lung, and the capillary, venous, and/or arterial microvasculature of the skin, defines a significant component of the underlying pathophysiology of severe COVID-19 [1,5]. The systemic nature of COVID-19 is reinforced by the findings of thrombotic livedoid purpura in the earlier study [1] and observed in three additional cases in the present study, along with additional reports detailing stroke and thrombotic emboli [3,11]. In this study, patients with severe COVID-19 demonstrated significant microvascular complement deposition in both thrombosed lesional and

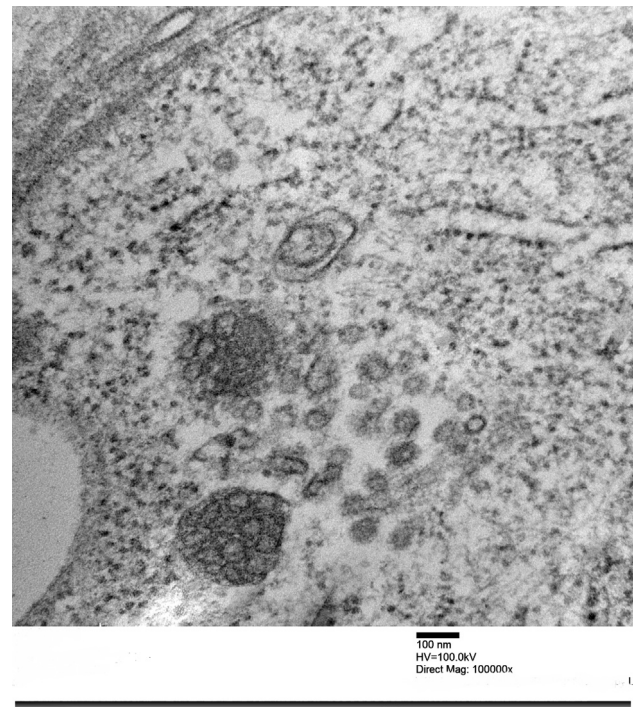


Fig. 7 EM findings in normal deltoid skin from a patient with fatal COVID-19. Deep dermal capillary vascular endothelial cells showing swelling, rough endoplasmic reticulum, intracytoplasmic lysosomes, and multivesicular bodies (arrows), representing a form of lysosomes along with a cluster of circular bodies with indistinct projections on the surface ranging from 45 to 55 nm in diameter, without a granular core (arrow heads) in direct contact with the cytosol, possibly indicating pseudovirions, derived from SARS-CoV-2 viral particles versus clathrin-coated vesicles. The classic SARS-CoV-2 intact virion surrounded by a membrane-bound vacuole and with its distinct beaded interior is not seen (uranyl nitrate and lead citrate, $\times 50,000$ and $\times 100,000$). COVID-19, coronavirus disease 2019; EM, electron microscopy; SARS-CoV-2, severe acute respiratory syndrome coronavirus 2.

normal-appearing nonlesional skin and subcutaneous fat. The extent of vascular C5b-9 deposition in patients with severe COVID-19 was to a degree that has been shown in

prior studies to signify systemic complement activation. Furthermore, the microvascular complement deposition was accompanied by histologic features characteristic for complement-mediated microvascular injury such as endothelial cell denudement, basement membrane zone reduplication, and intravascular thrombi most apparent in the deeper dermis and subcutaneous fat, where the microvascular complement deposition was greatest.

The presumed basis for this pattern of cutaneous vascular complement deposition and subsequent vascular injury is the ability of SARS-CoV-2 to activate the complement pathway systemically. We postulate that the mechanism of complement activation in COVID-19 is twofold. First, SARS-CoV-2 is known to use ACE2 as an entry point to certain cell types including those of lung, kidney, brain, and intestinal origin. This leads to reduced levels of ACE2 systemically and higher levels of angiotensin II than angiotensin 1–7 [12,13]. This imbalance can lead to reactive oxygen species in the endothelium and vasoconstriction; these in turn promote complement activation and thrombosis [14,15]. A second proposed mechanism lies in the activation of the MBL pathway by the glycosylated SARS-CoV-2 spike protein. Both of these mechanisms may be shared by the original SARS-CoV [16–19]. Jettisoned viral capsid microparticles that include the spike glycoprotein in the circulation can be endocytosed by ACE2+ endothelia that could result in complement activation via MBL activation without implying viral replication [20–22]. Second, there may be viremia inducing systemic MASP2-driven thrombosis and complement deposition by cleaving C4 and C2 [20,23], as suggested by the detection of coronavirus RNA in the plasma during SARS-CoV infection [24,25].

In this study, an association between cutaneous and subcutaneous microvascular complement deposition reflective of complement activation and SARS-CoV-2 docked protein within the endothelium was demonstrated. There was no evidence of viral replication in any of the skin samples studied based on the lack of viral RNA as detected by an ultrasensitive *in situ* method, which the manufacturer indicates can detect 1 SARS-CoV-2 genome per cell [9].

SARS-CoV-2 spike glycoprotein was found in ACE2-positive microvessels. Spike glycoprotein has certain binding sites on MBL, resulting in activation of MASP2. After MASP2 is activated, the C3 convertase is formed eventuating in the formation of C5b-9. When the MBL pathway is activated, there is the release of various factors that play a key role in activating the coagulation cascade and also providing an amplification loop for the alternative pathway. Other studies have also shown that endocytosed spike glycoprotein alone defining a pseudovirion without requiring an intact virus can directly interact with ACE2 [19]. The ultrastructural findings in the one case studied did not show any evidence of intact virions. The rounded structure was of smaller caliber, without any internal beading, indicative of the nucleocapsid, and was sitting

freely in the cytosol. The critical importance of recognizing these structures as not representing the virus has been emphasized in a recent editorial. They could represent clathrin-coated vesicles that are normal organelles, whereby their projections are in direct contact with the cytosol and are devoid of the dense dots inside the particles corresponding to the coiled nucleocapsid cut in cross section. Furthermore, coronaviruses have their projections extending inside membrane-bound vacuoles within the cells. One might also question whether or not these structures represent the endocytosed pseudovirions [26,27]. Given the parallel distribution of SARS-CoV-2 membrane, envelope, and spike glycoprotein, the capsid proteins likely travel as a unit and adhere to ACE2 via spike glycoprotein.

The data suggest that the subcutaneous fat of the skin may define an important site for endocytosed viral proteins because ACE2 was markedly expressed in the skin vasculature of the deeper dermis and subcutaneous fat. Thus, the findings of microvascular injury in apparently normal fat would therefore not be unexpected and provide credence to the pathophysiologic specificity of complement deposition. Obesity is a risk factor for severe COVID-19, although the exact link between obesity and the severity of disease has not been established. The significant degree of ACE2 expression in subcutaneous vessels allowing the docking of viral proteins could play a role in this association because the number of such microvessels would be in direct proportion to the amount of subcutaneous fat [28]. Existing data would suggest that the expansion of subcutaneous fat in adults is associated with a proangiogenic gene expression profile. Both capillary density and the ability of the subcutaneous fat to produce new capillaries appear to be linked with higher levels of vascular endothelial cell growth factors in individuals with obesity and without diabetes. Therefore, not only the overall amount of fat is increased but also the number of vessels per gram of fat is increased, and therefore, the fat in a patient with obesity and with severe COVID-19 is potentially a significant fuel for amplification of complement and coagulation pathways owing to the quantitative extent of complement activation [29]. Further studies beyond the scope of this article are needed to evaluate this possibility.

A critical downstream effect of extensive complement activation is the release of other factors that could lead to a systemic increase in coagulopathic events as evidenced by the presence of widespread multiorgan thrombosis and massively elevated levels of D-dimers. For instance, both complement anaphylatoxins, C3a and C5a, in the complement system can activate platelets and increase the production of tissue factor, respectively [30–32]. For example, MASP2 is thrombin generating [33]. Furthermore, as complement destroys the endothelium, the procoagulant von Willebrand factor and FVIII are released, sometimes in high amounts [34,35]. Interestingly, von Willebrand factor activity is dictated by blood type, with type AB having ~125% activity and type O having ~75% of A and B

blood type, which might explain recent reports linking type O blood to better outcomes [36]. This is only part of the interplay for reciprocally, thrombin, FXa, and FIXa can act to trigger the complement cascade by acting as C3 and C5 convertases [32,37]. In addition, the alternative pathway is activated by components of complement activation contributing to the distant microvascular injury that occurs. The loss of ACE2 contributes to this prothrombotic state by creating an outsized angiotensin II-to-angiotensin 1–7 ratio. This leads to clot-fostering vasoconstriction and prothrombotic oxidation through Nox-2 [38,39]. Taken together, COVID-19 is a strongly prothrombotic disease.

The deltoid biopsy area is the recommended preferred site for a skin biopsy in evaluating for evidence of systemic complement activation to reduce the incidence of false positivity for complement deposition. In particular, sun exposure is an independent activator of the complement pathway especially in the setting of photosensitizing agents, and hence, sun-exposed biopsy sites are not desirable [40]. Lower extremity biopsies are also not ideal due to the role of hydrostatic pressure in trapping of immune complexes, which may result in subclinical classic complement pathway activation [41].

In summary, the skin represents a potentially important site for complement activation owing to released viral proteins binding to cutaneous and subcutaneous ACE2-positive vessels. Additional studies are needed to determine if this viral induced process in the skin is a major factor in the hypercoagulable state and cytokine storm that defines severe COVID-19.

Acknowledgments

C.M., G.J.N., and J.J.M. wrote the article and designed the research study. All authors but A.J.D. performed the research and contributed essential, consented samples and know-how. C.M. and G.J.N. analyzed the data. J.L., C.M., A.N.C., G.J.N., A.J.D., J.H., and J.J.M. revised and edited the manuscript. The authors thank Dr. Margaret Nuovo for help with the photomicrographs.

References

- [1] Magro C, Mulvey JJ, Berlin D, et al. Complement associated microvascular injury and thrombosis in the pathogenesis of severe COVID-19 infection: a report of five cases. *Transl Res* 2020. <https://doi.org/10.1016/j.trsl.2020.04.007>.
- [2] WHO. Report of the WHO-China joint mission on coronavirus disease 2019 (COVID-19). 2020.
- [3] Mao L, Jin H, Wang M, et al. Neurologic manifestations of hospitalized patients with coronavirus disease 2019 in Wuhan, China. *JAMA Neurol* 2020. <https://doi.org/10.1001/jamaneurol.2020.1127>.
- [4] Zhou F, Yu T, Du R, et al. Clinical course and risk factors for mortality of adult inpatients with COVID-19 in Wuhan, China: a retrospective cohort study. *Lancet* 2020;395:1054–62. [https://doi.org/10.1016/S0140-6736\(20\)30566-3](https://doi.org/10.1016/S0140-6736(20)30566-3).
- [5] Magro C, Mulvey JJ, Laurence J, et al. The differing pathophysiologies that underlie COVID-19 associated perniois and thrombotic retiform purpura: a case series. *Br J Dermatol* 2020;194:15. <https://doi.org/10.1111/bjd.19415>.
- [6] Magro CM, Momtahan S, Mulvey JJJJ, Yassin AHAH, Kaplan RB, Laurence JCJC. Role of the skin biopsy in the diagnosis of atypical hemolytic uremic syndrome. *Am J Dermatopathol* 2015;37. <https://doi.org/10.1097/DAD.0000000000000234>.
- [7] Magro CM, Dysrsen ME. The use of C3d and C4d immunohistochemistry on formalin-fixed tissue as a diagnostic adjunct in the assessment of inflammatory skin disease. *J Am Acad Dermatol* 2008; 59:822–33. <https://doi.org/10.1016/j.jaad.2008.06.022>.
- [8] Vasil KE, Magro CM. Cutaneous vascular deposition of C5b-9 and its role as a diagnostic adjunct in the setting of diabetes mellitus and porphyria cutanea tarda. *J Am Acad Dermatol* 2007. <https://doi.org/10.1016/j.jaad.2006.05.013>.
- [9] Nuovo GJ. In situ molecular pathology and Co-expression analyses. 2013. <https://doi.org/10.1016/C2011-0-05539-4>.
- [10] Mansfield JR. Cellular context in epigenetics: quantitative multicolor imaging and automated per-cell analysis of miRNAs and their putative targets. *Methods* 2010;52:271–80. <https://doi.org/10.1016/j.ymeth.2010.10.001>.
- [11] Xie Y, Wang X, Yang P, Zhang S. COVID-19 complicated by acute pulmonary embolism. *Radiol Cardiothorac Imaging* 2020. <https://doi.org/10.1148/ryct.2020200067>.
- [12] Nuovo GJ, Magro C, Mikhail A. Cytologic and molecular correlates of SARS-CoV-2 infection of the nasopharynx. *Ann Diagn Pathol* 2020 Jul 7;48:151565. <https://doi.org/10.1016/j.anndiagpath.2020.151565>. Epub ahead of print. PMID: 32659620.
- [13] Nuovo G. False-positive results in diagnostic immunohistochemistry are related to horseradish peroxidase conjugates in commercially available assays. *Ann Diagn Pathol* 2016 Dec;25:54–9. <https://doi.org/10.1016/j.anndiagpath.2016.09.010>. Epub 2016 Sep 26.
- [14] Shagdarsuren E, Wellner M, Braesen JH, et al. Complement activation in angiotensin II-induced organ damage. *Circ Res* 2005. <https://doi.org/10.1161/01.RES.0000182677.89816.38>.
- [15] Collard CD, Väkevä A, Morrissey MA, et al. Complement activation after oxidative stress: role of the lectin complement pathway. *Am J Pathol* 2000. [https://doi.org/10.1016/S0002-9440\(10\)65026-2](https://doi.org/10.1016/S0002-9440(10)65026-2).
- [16] Gralinski LE, Sheahan TP, Morrison TE, et al. Complement activation contributes to severe acute respiratory syndrome coronavirus pathogenesis. *mBio* 2018. <https://doi.org/10.1128/mBio.01753-18>.
- [17] Walls AC, Park Y-J, Tortorici MA, Wall A, McGuire AT, Velesler D. Structure, function, and antigenicity of the SARS-CoV-2 spike glycoprotein. *Cell* 2020. <https://doi.org/10.1016/j.cell.2020.02.058>.
- [18] Ip WKE, Chan KH, Law HKW, et al. Mannose-binding lectin in severe acute respiratory syndrome coronavirus infection. *J Infect Dis* 2005;191:1697–704.
- [19] Ou X, Liu Y, Lei X, et al. Characterization of spike glycoprotein of SARS-CoV-2 on virus entry and its immune cross-reactivity with SARS-CoV. *Nat Commun* 2020;11. <https://doi.org/10.1038/s41467-020-15562-9>.
- [20] Jalal D, Renner B, Laskowski J, et al. Endothelial microparticles and systemic complement activation in patients with chronic kidney disease. *J Am Heart Assoc* 2018. <https://doi.org/10.1161/JAHA.117.007818>.
- [21] Liu Y, Zhang R, Qu H, Wu J, Li L, Tang Y. Endothelial microparticles activate endothelial cells to facilitate the inflammatory response. *Mol Med Rep* 2017;15:1291–6. <https://doi.org/10.3892/mmr.2017.6113>.
- [22] Dignat-George F, Boulanger CM. The many faces of endothelial microparticles. *Arterioscler Thromb Vasc Biol* 2011. <https://doi.org/10.1161/ATVBAHA.110.218123>.
- [23] Turner MW. The role of mannose-binding lectin in health and disease. *Mol Immunol* 2003. [https://doi.org/10.1016/S0161-5890\(03\)00155-X](https://doi.org/10.1016/S0161-5890(03)00155-X).

- [24] Wang WK, Fang CT, Chen HL, et al. Detection of severe acute respiratory syndrome coronavirus RNA in plasma during the course of infection. *J Clin Microbiol* 2005;43:962–5. <https://doi.org/10.1128/JCM.43.2.962-965.2005>.
- [25] Magro CM, Poe JC, Kim C, et al. Degos disease: a C5b-9/interferon- α -mediated endotheliopathy syndrome. *Am J Clin Pathol* 2011. <https://doi.org/10.1309/AJCP66QIMFARLZKI>.
- [26] Miller SE, Brealey JK. Visualization of putative coronavirus in kidney. *Kidney Int* 2020;98:231–2. <https://doi.org/10.1016/j.kint.2020.05.004>.
- [27] Miller SE, Goldsmith CS. Caution in identifying coronaviruses by electron microscopy. *J Am Soc Nephrol* 2020. <https://doi.org/10.1681/ASN.2020050755>.
- [28] Dietz W, Santos-Burgoa C. Obesity and its implications for COVID-19 mortality. *Obesity (Silver Spring)* 2020. <https://doi.org/10.1002/oby.22818>.
- [29] Corvera S, Gealekman O. Adipose tissue angiogenesis: impact on obesity and type-2 diabetes. *Biochim Biophys Acta (BBA) - Mol Basis Dis* 2014;1842:463–72. <https://doi.org/10.1016/j.bbadis.2013.06.003>.
- [30] Subramaniam S, Jurk K, Hobohm L, et al. Distinct contributions of complement factors to platelet activation and fibrin formation in venous thrombus development. *Blood* 2017;129:2291–302. <https://doi.org/10.1182/blood-2016-11-749879>.
- [31] Ruf W. Links between complement activation and thrombosis. *Blood* 2019;134. <https://doi.org/10.1182/blood-2019-121113>. SCI-40-SCI-40.
- [32] Nilsson H-L, Gebhard F, Lambris JD, et al. Complement and coagulation systems molecular intercommunication between the. *J Immunol Ref* 2010;185:5628–36. <https://doi.org/10.4049/jimmunol.0903678>.
- [33] Krarup A, Wallis R, Presanis JS, Gál P, Sim RB. Simultaneous activation of complement and coagulation by MBL-associated serine protease 2. *PloS One* 2007;2. <https://doi.org/10.1371/journal.pone.0000623>.
- [34] Blann AD, McCollum CN. von Willebrand factor, endothelial cell damage and atherosclerosis. *Eur J Vasc Surg* 1994;8:10–5. [https://doi.org/10.1016/S0950-821X\(05\)80112-4](https://doi.org/10.1016/S0950-821X(05)80112-4).
- [35] Reinhart K, Bayer O, Brunkhorst F, Meisner M. Markers of endothelial damage in organ dysfunction and sepsis. *Crit Care Med* 2002. <https://doi.org/10.1097/00003246-200205001-00021>.
- [36] Ellinghaus D, Degenhardt F, Bujanda L, et al. Genomewide association study of severe covid-19 with respiratory failure. *N Engl J Med* 2020. <https://doi.org/10.1056/NEJMoa2020283>. NEJMoa2020283.
- [37] Speth C, Rambach G, Würzner R, et al. Complement and platelets: mutual interference in the immune network. *Mol Immunol* 2015. <https://doi.org/10.1016/j.molimm.2015.03.244>.
- [38] Lynch SM, Frei B, Morrow JD, et al. Vascular superoxide dismutase deficiency impairs endothelial vasodilator function through direct inactivation of nitric oxide and increased lipid peroxidation. *Arterioscler Thromb Vasc Biol* 1997. <https://doi.org/10.1161/01.ATV.17.11.2975>.
- [39] Chu AJ. Tissue factor, blood coagulation, and beyond: an overview. *Int J Inflamm* 2011;2011:1–30. <https://doi.org/10.4061/2011/367284>.
- [40] Giang J, Seelen MAJ, Van Doorn MBA, Rissmann R, Prens EP, Damman J. Complement activation in inflammatory skin diseases. *Complement Act Inflamm Ski Dis Front Immunol* 2018;9:639. <https://doi.org/10.3389/fimmu.2018.00639>.
- [41] Shishkova NV, Donchenko LI, Barbashova BI, Ulyanova EV. High hydrostatic pressure effect on activity of circulating immune complex formation in blood serum. In: *Adv. High Press. Biosci. Biotechnol.* Berlin, Heidelberg: Springer; 1999. p. 239–42. https://doi.org/10.1007/978-3-642-60196-5_53.